

Detectable environmental effects in GW190521-like black-hole binaries with LISA

Alexandre Toubiana,^{1,2} Laura Sberna,³ Andrea Caputo,^{4,5,6} Giulia Cusin,⁷ Sylvain Marsat,¹ Karan Jani,⁸ Stanislav Babak,^{1,9} Enrico Barausse,^{10,11} Chiara Caprini,¹ Paolo Pani,¹² Alberto Sesana,^{13,14} and Nicola Tamanini¹⁵

¹*APC, AstroParticule et Cosmologie, Université de Paris, CNRS, F-75013 Paris, France*

²*Institut d'Astrophysique de Paris, CNRS & Sorbonne Universités, UMR 7095, 98 bis bd Arago, 75014 Paris, France*

³*Perimeter Institute, 31 Caroline St N, Ontario, Canada*

⁴*Instituto de Física Corpuscular, Universidad de Valencia and CSIC, Edificio Institutos Investigacion, Catedrático Jose Beltrán 2, Paterna, 46980 Spain*

⁵*School of Physics and Astronomy, Tel-Aviv University, Tel-Aviv 69978, Israel*

⁶*Department of Particle Physics and Astrophysics, Weizmann Institute of Science, Rehovot 7610001, Israel*

⁷*Université de Genève, Département de Physique Théorique and Centre for Astroparticle Physics, 24 quai Ernest-Ansermet, CH-1211 Genève 4, Switzerland*

⁸*Department Physics and Astronomy, Vanderbilt University, 2301 Vanderbilt Place, Nashville, TN, 37235, USA*

⁹*Moscow Institute of Physics and Technology, Dolgoprudny, Moscow region, Russia*

¹⁰*SISSA, Via Bonomea 265, 34136 Trieste, Italy & INFN, Sezione di Trieste*

¹¹*IFPU - Institute for Fundamental Physics of the Universe, Via Beirut 2, 34014 Trieste, Italy*

¹²*Dipartimento di Fisica, "Sapienza" Università di Roma & Sezione INFN Roma1, Piazzale Aldo Moro 5, 00185, Roma, Italy*

¹³*Department of Physics G. Occhialini, University of Milano - Bicocca, Piazza della Scienza 3, 20126 Milano, Italy*

¹⁴*National Institute of Nuclear Physics INFN, Milano - Bicocca, Piazza della Scienza 3, 20126 Milano, Italy*

¹⁵*Max-Planck-Institut für Gravitationsphysik, Albert-Einstein-Institut, Am Mühlenberg 1, 14476 Potsdam-Golm, Germany.*

GW190521 is the compact binary with the largest masses observed to date, with at least one in the pair-instability gap. This event has also been claimed to be associated with an optical flare observed by the Zwicky Transient Facility in an Active Galactic Nucleus (AGN), possibly due to the post-merger motion of the merger remnant in the AGN gaseous disk. We show that the Laser Interferometer Space Antenna (LISA) will detect up to ten of such gas-rich black hole binaries months to years before their detection by LIGO/Virgo-like interferometers, localizing them in the sky within $\approx 1 \text{ deg}^2$. LISA will also measure directly deviations from purely vacuum and stationary waveforms, arising from gas accretion, dynamical friction, and orbital motion around the AGN's massive black hole (acceleration, strong lensing, and Doppler modulation). LISA will therefore be crucial to alert and point electromagnetic telescopes ahead of time on this novel class of gas-rich sources, to gain direct insight on their physics, and to disentangle environmental effects from corrections to General Relativity that may also appear in the waveforms at low frequencies.

GW190521 is the most massive compact binary merger observed by the LIGO/Virgo Collaboration (LVC) to date, with progenitor black-hole (BH) masses of $85^{+21}_{-14} M_{\odot}$ and $66^{+17}_{-18} M_{\odot}$ [1, 2]. The larger BH lies right in the pair-instability gap $\sim [50, 130] M_{\odot}$ [3–5], calling for interpretations beyond standard stellar-evolution models. A viable channel to produce such massive BHs is via repeated mergers (which would also explain the large misaligned spins of GW190521 [1, 2]), e.g. in stellar clusters [6–8] or in active galactic nuclei (AGNs) [9–11]. While [2] suggests that repeated mergers might be rare in globular clusters, due to BH ejection by gravitational recoil, nuclear star clusters have higher escape velocities and more efficiently retain merger remnants. Alternatively, GW190521 may have formed in an AGN disk, where mass segregation/dynamical friction (DF) favor BH accumulation near the center (enhancing merger rates) and their growth by mergers/accretion [9–13]. The large GW190521 masses may also be consistent with metal-free, population III star progenitors [14] (see also [15, 16]). Other less standard scenarios include beyond-Standard-Model physics [17], primordial BHs [18], boson stars [19], and extensions of General Relativity (GR) [20]. Finally, [21] note that there is a non-negligible probability of GW190521 being a “straddling” binary, with components below and above the pair-instability gap. Although some analyses [22–24] suggest

that eccentric waveforms might fit the data better, supporting a dynamical origin in a dense environment, the formation of GW190521 remains mysterious.

Remarkably, the Zwicky Transient Facility observed an optical flare (ZTF19abanrhr), interpreted as coming from the kicked GW190521 BH merger remnant moving in an AGN disk [25]. If confirmed, this would be the first electromagnetic counterpart to a BH coalescence (see however [26, 27]). The flare occurred ~ 34 days after GW190521 (the delay being ascribed to the remnant's recoil) in AGN J124942.3+344929 at redshift $z = 0.438$. If the flare is indeed associated with GW190521 and due to the remnant's recoil in the AGN disk, [25] finds a total binary mass $\sim 150 M_{\odot}$, kick velocity $\sim 200 \text{ km/s}$ at $\sim 60 \text{ deg}$ from the disk's midplane, disk aspect ratio (height to galactocentric radius) $H/a \sim 0.01$, and gas density $\rho \sim 10^{-10} \text{ g/cm}^3$. They also argue that the binary is most likely located in a disk migration trap (galactocentric distance $a \sim 700 GM/c^2$, with $M \sim 10^8 - 10^9 M_{\odot}$ the mass of the AGN's central BH), where gas torques vanish and binaries accumulate as they migrate inwards [28]. While the GW190521–ZTF19abanrhr association is debated [29], the results presented below do not rely on it, but only assume that GW190521-like systems reside in gas-rich environments (e.g. AGNs [9–13]).

Months to years before merging in the LIGO/Virgo

band, BH binaries with masses of at least a few tens M_\odot spiral in the mHz band of the Laser Interferometer Space Antenna (LISA) [30], a gravitational-wave (GW) spaceborne experiment scheduled for 2034. Observing several years of inspiral with LISA would permit estimating the source parameters with high precision [31–33] – e.g. the chirp mass and distance to fractional errors $\sim 10^{-4}$ and ~ 0.4 , respectively, the sky position below $\sim 1 \text{ deg}^2$ – and, crucially, it would allow for predicting the coalescence time within a minute, weeks before the signal is detected from Earth. This would permit alerting electromagnetic telescopes in advance, pointing them at smaller sky regions, and looking for electromagnetic counterparts [31] *coincident* with the coalescence. Moreover, GR extensions typically predict low-frequency corrections to the GW phase, e.g. vacuum dipole emission at -1 post-Newtonian (PN) order, which will be tested to exquisite precision by LISA inspiral observations [34–36].

We show below that LISA might observe several gas-rich, high-mass BH binaries. Besides observing these sources beforehand and localizing them accurately [38], LISA will also detect environmental (i.e. non-vacuum [37]) effects directly in the GW signal, namely gas accretion/DF on the component BHs, the binary’s acceleration around the AGN’s BH, and possibly the Doppler modulation and the lensing/Shapiro time delay from the central BH. These effects may jeopardize low-frequency tests of GR (with which they may be degenerate), but may help localize the source by correlating with AGN catalogs. Henceforth, we use units where $G = c = 1$.

Event rates. Assuming a binary population with parameters drawn from the LVC posteriors, Ref. [2] estimates the comoving merger rate of GW190521-like systems as $0.13^{+0.30}_{-0.11} \text{ yr}^{-1} \text{ Gpc}^{-3}$. With the same hypotheses, LISA will observe 1–10 such systems, depending on the high-frequency laser noise, the mission lifetime, and the operation duty cycle, out to $z \approx 0.5$ (for more details see [38]). Note that, if GW190521 lies at the low-mass end of a heavy-BH population extending beyond $100M_\odot$, LISA rates would be significantly higher (because in the $(10 - 10^3)M_\odot$ range the LISA horizon distance is $\propto \mathcal{M}^{5/3}$, with \mathcal{M} the source-frame chirp mass [32]). Indeed, if we conservatively assume a Salpeter mass function extending to $200M_\odot$, the inferred LVC rate would boost LISA detections by about an order of magnitude (see also [39]).

Detectability of environmental effects. We model accretion from the AGN gas disk by the Eddington ratio $f_{\text{Edd}} \equiv \dot{m}/\dot{m}_{\text{Edd}}$ between the mass accretion rate \dot{m} of either BH and $\dot{m}_{\text{Edd}} \equiv L_{\text{Edd}}/\eta$, with L_{Edd} the Eddington luminosity and the radiative efficiency set to $\eta \approx 0.1$. The mass growth of the BHs ($i = 1, 2$) is $m_i(t) = m_i(0) \exp(f_{\text{Edd}} t/\tau_S)$, with $\tau_S = 4.5 \times 10^7 \text{ yr}$ the Salpeter time. The phase term in the Fourier-domain GW signal $\tilde{h} \sim |\tilde{h}| e^{i\tilde{\phi}}$ induced by the mass growth can be evaluated in the stationary phase approximation at leading PN

order [40]:

$$\tilde{\phi}_{\text{accretion}} \approx -f_{\text{Edd}} (8\xi + 15) \frac{75 \mathcal{M}(1+z)}{851968 \tau_S} [\pi f \mathcal{M}(1+z)]^{-13/3}, \quad (1)$$

with f the observed GW frequency, z the redshift at coalescence, and $\xi \sim \mathcal{O}(1)$ a factor parametrizing the drag due to the momentum transferred by the accreted gas [40], which we conservatively set to zero.

The binary’s center of mass (CoM) acceleration around the central massive BH also modifies the waveform, as studied in [41–43] for CoM accelerations almost constant during the observation period. Neglecting the universe expansion, the phase correction reads [41–43]

$$\tilde{\phi}_{\text{acceleration}} \approx \frac{25 \mathcal{M}}{65536} \dot{v}''(t_c) [\pi f \mathcal{M}(1+z)]^{-13/3}, \quad (2)$$

where \dot{v}'' is the acceleration projected on the line of sight, computed at coalescence. For quasi-circular galactocentric orbits, $\dot{v}'' \approx (3.2 \times 10^{-11} \text{ m/s}^2) \epsilon$, where [41]

$$\epsilon = \left(\frac{v_{\text{orb}}}{100 \text{ km/s}} \right)^2 \frac{10 \text{ kpc}}{a} \cos \psi, \quad (3)$$

with v_{orb} the orbital velocity around the central BH, and ψ the angle between the line of sight and the acceleration. Since $\cos \psi = \cos \iota \sin(\Omega t + \phi_0)$ (with ι the inclination angle of the line of sight relative to the AGN disk, $\Omega = \sqrt{M}/a^{3/2}$, and ϕ_0 the initial phase), the assumption of constant acceleration only holds at sufficiently large galactocentric distances a (i.e. low Ω). We will verify this assumption a posteriori (and relax it) later.

Eqs. (1)–(2) show that accretion and (constant) acceleration are degenerate, since they both appear at -4 PN order [37, 40, 41, 44] (though accretion always yields a negative phase contribution, while acceleration can give contributions of either sign). Both effects can be included in the waveform via a phenomenological PN term $\tilde{\phi}_{-4\text{PN}} = \varphi_{-4} [\pi f \mathcal{M}(1+z)]^{-13/3}$ [45], with φ_{-4} related to f_{Edd} and ϵ for accretion and acceleration, respectively.

We also consider the DF from gas with density ρ surrounding the binary. Assuming that the binary’s CoM is approximately comoving with the gas, DF exerts a drag force on each BH (opposite to the BH’s velocity \vec{v}_i in the CoM frame), $F_{\text{DF},i} = 4\pi\rho(Gm_i)^2 I(r_i, v_i)/v_i^2$, where r_i is the distance of the BH from the CoM, and we assume $v_i \gg c_s$ (with c_s the gas speed of sound; note that v_i is relativistic when the binary is in the LISA band). We use the analytic expression of the “Coulomb logarithm” $I(r, v)$ provided in [46], which was validated against simulations up to $v_i/c_s = 8$, but which we extrapolate further (see also [47]).

We assume here $c_s \approx v_{\text{orb}}(H/a)$ [48], with $H/a \sim 0.01$ [25]. Following [46] (see also [49–51]), we only include the effect of the wake created by each BH on itself, and neglect the companion’s [52]. For $f \lesssim 0.3 \text{ Hz}$ this is a good approximation, since the orbital separation of GW190521 in the LISA band is larger than the wake’s size. In the adiabatic

approximation, the DF-induced phase correction first enters at -5.5PN order:

$$\tilde{\phi}_{\text{DF}} \approx -\rho \frac{25\pi(3\nu-1)\mathcal{M}^2(1+z)^2}{739328\nu^2} \gamma_{\text{DF}} [\pi f \mathcal{M}(1+z)]^{-16/3}, \quad (4)$$

with $\gamma_{\text{DF}} = -247 \log(f/f_{\text{DF}}) - 39 + 304 \log(20) + 38 \log(3125/8)$ and $f_{\text{DF}} = c_s/[22\pi(m_1+m_2)]$, being $\nu = m_1 m_2 / (m_1 + m_2)^2$ the symmetric mass ratio.

In Fig. 1 we show the distribution of errors – produced with the augmented Fisher formalism of [33] – for the Eddington rate f_{Edd} , the acceleration parameter ϵ , and the gas density ρ , (normalized to $\rho_0 = 10^{-10} \text{ g cm}^{-3}$ [25]). We use $f_{\text{Edd}} = \rho = \epsilon = 0$ as injections, i.e. the distributions represent optimistic upper bounds on the parameters. We use the samples released by the LVC, for the NRSur7dq4 model [53] and, for each sample, draw sky location and polarization randomly. The extra terms of Eqs. (1), (2), and (4) were added to PhenomD waveforms [54, 55] one at a time, and we accounted for the antenna motion during observations as done, e.g., in [33, 56, 57]. We consider detections by LISA

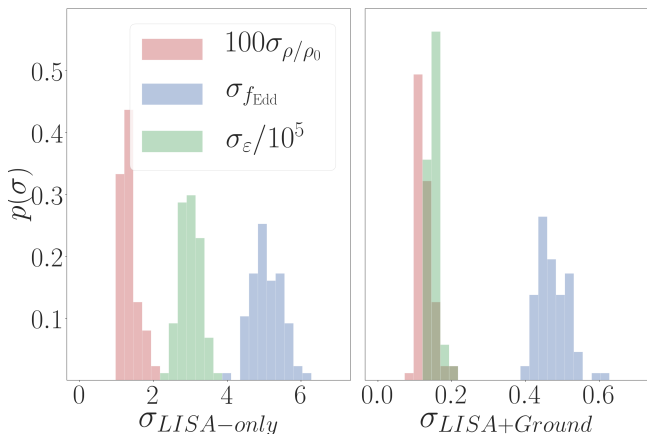


FIG. 1. Distribution of Fisher-matrix errors on environmental effects with LISA alone or in combination with ground detectors.

alone, and in combination with ground interferometers. In the latter case, we assume that the masses, spins, and merger time can be measured by ground detectors, which reduces the parameter-space dimension.

We find that LISA alone can detect super-Eddington accretion rates ($f_{\text{Edd}} \geq 5$), which may be typical in dense environments [58], and acceleration parameters $\epsilon \geq 3 \times 10^5$, corresponding to $a \approx 1 \text{ pc}$ for $M = 10^8 M_\odot$. The DF effect is even stronger, with ρ/ρ_0 constrained at percent level. All errors improve by about an order of magnitude with multiband detections (e.g. sub-Eddington accretion rates become measurable).

Besides considering environmental effects one by one, we focus on a single system compatible with the LVC posteriors and perform a Markov-Chain-Monte-Carlo analysis [59] similar to that of [33], injecting non-zero values (plausible for sources in AGNs) for all environmental effects: $f_{\text{Edd}} = 5$,

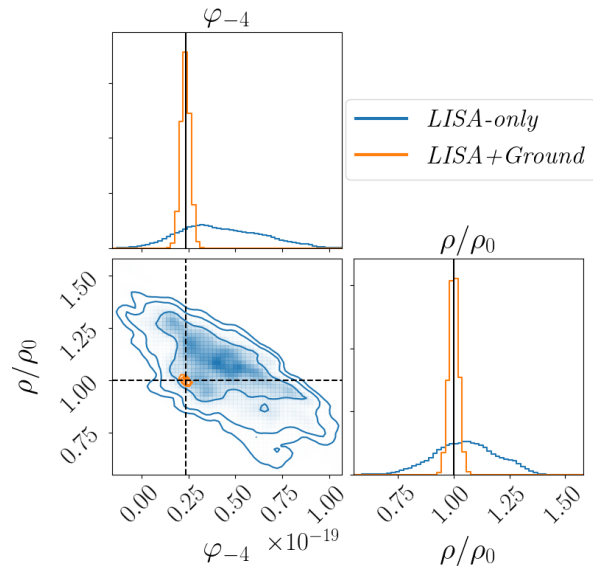


FIG. 2. Posterior distribution of gas density and -4PN phase term (corresponding to constant acceleration/accretion), with their 68%, 90% and 99% confidence contours. Black lines indicate the injected values.

$\epsilon = 3.2 \times 10^6$ (corresponding to $a \approx 0.4 \text{ pc}$ for $M = 10^8 M_\odot$) and $\rho = \rho_0$. Fig. 2 shows the posterior distributions for the density (ρ/ρ_0) and the parameter φ_{-4} accounting for acceleration/accretion. Both parameters can be measured well, since they appear at different (negative) PN orders. Note that the sign of φ_{-4} can help distinguish accretion ($\varphi_{-4} < 0$) from acceleration (φ_{-4} of either sign).

We have verified a posteriori the assumption of constant acceleration, i.e. for the results above the systematic error produced by the variation of ϵ over the observation time T_{obs} is negligible with respect to the statistical error. For $a \lesssim 0.25 \text{ pc} [M/(10^8 M_\odot)]^{3/7} [T_{\text{obs}}/(6\text{yr})]^{2/7}$ (i.e. orbital periods $T \lesssim 1200 \text{ yr} [M/(10^8 M_\odot)]^{1/7} [T_{\text{obs}}/(6\text{yr})]^{3/7}$), however, this may no longer be true. This is the case, e.g., if GW190521 lies in a disk migration trap. Ref. [25] estimates the trap distance from the central BH as $a \sim 700M$, corresponding to $T \sim 1.8 \text{ yr}$, i.e. the acceleration cannot be assumed constant over the observation time.

We can estimate the effect of non-constant acceleration as follows. Ignoring cosmic expansion, the observed signal is $s(t) = h(t + d^{\text{II}}(t))$, with $h(t)$ the source-frame strain. The delay $d^{\text{II}}(t)$ arises from the change in the source distance due to the orbital motion, and is given by the projection of the orbit on the line of sight: $d^{\text{II}}(t) = a \cos i \sin(\Omega t + \phi_0)$. This time-varying delay produces an oscillating Doppler modulation $\phi_{\text{Doppler}} \sim 2\pi f d^{\text{II}}$ of the observed signal. The magnitude of this phase is of order

$$2\pi f a \sim 2 \times 10^4 \text{ rad} \left(\frac{M}{10^8 M_\odot} \right) \left(\frac{f}{10 \text{ mHz}} \right) \left(\frac{a}{700M} \right). \quad (5)$$

This effect strongly impacts the signal, dominating over

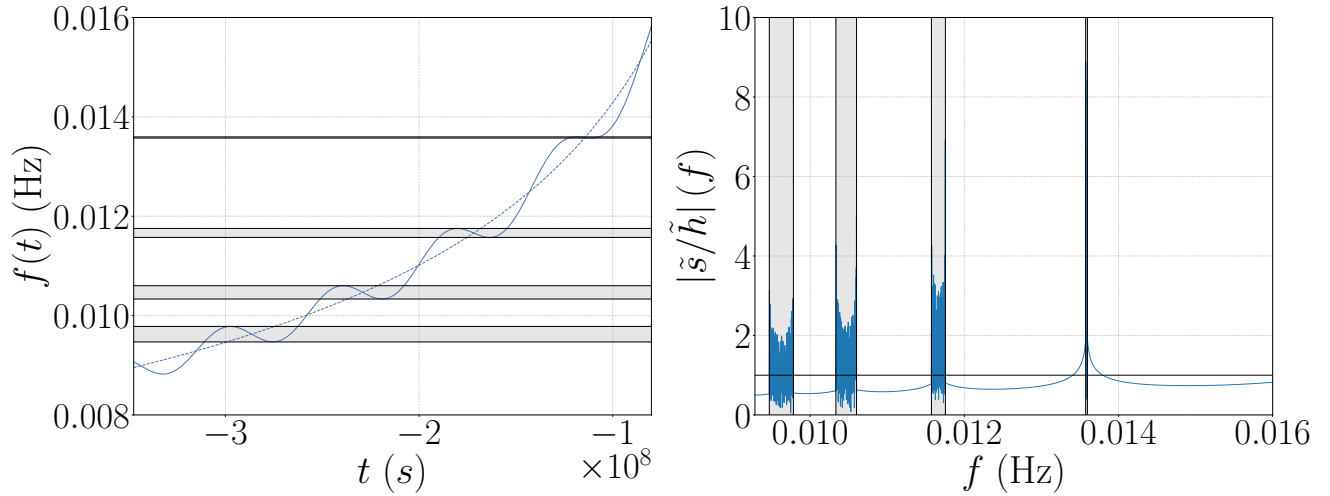


FIG. 3. Doppler modulations of the GW signal due to the motion around the central BH. The left panel shows the time-frequency track of the modulated signal (solid line) compared to the non-modulated one (dashed). The coalescence is at $t = 0$. The right panel shows the amplitude of the Fourier-domain transfer function $|\tilde{s}/\tilde{h}|(f)$, with a horizontal line at 1. In both panels, the shaded bands show the frequency bands where the time-to-frequency map becomes multi-valued.

the Doppler modulation produced by the LISA motion (≈ 30 rad), which happens on comparable timescales. The GW frequency suffers redshifts/blueshifts as the binary's CoM moves away from/toward LISA, as shown in Fig. 3. These modulations dominate over the GW-driven chirp rate, leading to a multi-valued time-to-frequency map in the shaded bands of Fig. 3, where chirping and anti-chirping parts of the signal are superposed. This strongly affects the Fourier-domain observed signal $\tilde{s}(f)$, with the transfer function amplitude $|\mathcal{T}(f)| = |\tilde{s}(f)/\tilde{h}(f)|$ showing interference patterns in the shaded bands. The impact on detection and parameter estimation is under study [38].

Another potentially detectable effect – particularly for edge-on AGN disks – is the strong lensing of the GW signal by the central BH, which occurs at scales given by the Einstein radius,

$$r_E \simeq (4MD_A)^{1/2} = (4Ma \cos i \sin(\Omega t + \phi_0))^{1/2}, \quad (6)$$

where we assume $a \ll D_A$, with D_A the angular diameter distance to the lens. Significant lensing occurs when the source passes within $\sim r_E$ from the lens, and the lensing probability is thus the fraction of time (during a full orbit around the central BH) for which this happens [60, 61]. A GW190521-like event in an AGN disk's migration trap falls either in the repeating-lens regime or in the slowly-moving lens regime defined e.g. in [61], depending on the observation time T_{obs} and M . The probability of strong lensing is (see Fig. 4)

$$P_{\text{lens}} = \text{Min} \left[\frac{10^{12} T_{\text{obs}}}{2 \text{ yr}} \left(\frac{a}{M} \right)^{-3/2} \frac{M_{\odot}}{M}, 1 \right] \frac{2}{\pi} \arcsin \left[2 \sqrt{\frac{M}{a}} \right]. \quad (7)$$

Strong lensing also affects the observed waveform directly. For a plane wave, the lensed signal (in real space) is given by

$$h^L(t) = F(f, t) h(t), \quad (8)$$

in terms of the the amplification factor $F(f, t)$. For a point-like lens in the geometric-optics approximation [62, 63],

$$F(f, t) = |\mu_+|^{1/2} - i|\mu_-|^{1/2} e^{2\pi i f \Delta t}, \quad (9)$$

where the magnification of each image, $\mu_{\pm} = 1/2 \pm (y^2 + 2)/(2y\sqrt{y^2 + 4})$, depends on time through the lensing parameter $y \equiv b/r_E$, with b the impact parameter. The time delay between two images is $\Delta t = \Delta t_{\text{fid}} \left[y/2 \sqrt{y^2 + 4} + \ln \left((\sqrt{y^2 + 4} + y)/(\sqrt{y^2 + 4} - y) \right) \right]$ where $\Delta t_{\text{fid}} \simeq 2 \times 10^{-5} (1 + z) M/M_{\odot} \text{sec}$. Periodic passages of the orbit behind the central massive BH will produce repeated interference patterns on the observed waveform. From Eq. (8), one sees that besides rescaling the waveform amplitude, strong lensing also yields an additive correction to the phase. For a plane wave, the latter is simply $\phi_{\text{SL}} = \text{Arg}[F(f, t)]$. We have checked, however, that this dephasing is typically smaller than the Doppler modulation described above (c.f. [38] for details).

Discussion. If GW190521-like events are confirmed to occur in dense gaseous environments, this novel class of GW sources may provide a unique multimessenger probe of AGN properties. By detecting the inspiral of these binaries months/years before their coalescence in the band of ground-based detectors [38], LISA will be crucial to localize potential electromagnetic counterparts and to measure the binary parameters with exquisite precision, but also to uncover non-vacuum effects. The latter can provide complementary information on the astrophysical environment

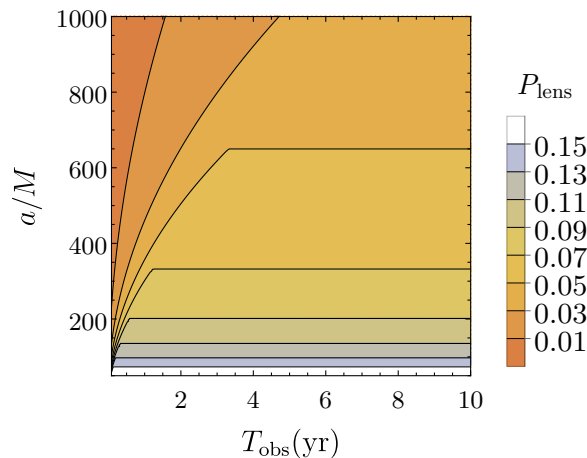


FIG. 4. Lensing probability as function of observation time, T_{obs} , and galactocentric distance, a/M , for $M = 10^8 M_{\odot}$.

of these sources, and may help improve their localization by correlating with AGN maps.

Accounting for environmental effects is also crucial to detect possible corrections to GR [37]. Effects like extra dimensions or a time-varying Newton constant enter the inspiral waveform at -4PN order [64], being thus degenerate with accretion or acceleration. Other effects, like vacuum dipole emission, also appear at negative PN orders [34]. If negative PN corrections are measured by standard parametrized tests [45], the detection of an electromagnetic counterpart in the LISA sky-position errorbox would favor an environmental origin over a beyond-GR one.

Given these tantalizing prospects, dedicated simulations would be needed to carefully describe environmental effects in binaries, accounting e.g. for radiative transfer and outflows that may affect DF and accretion [58, 65], and modeling strong accelerations in relativistic binaries accurately [38]. Relativistic corrections might also impact the signal, if the binary is close to the central BH (note that $a \approx 700M$ corresponds to $v_{\text{orb}} \approx 0.04$). These include orbital periastron precession, spin-orbit [66] and spin-spin [67] precession, and gravitational redshift. The Shapiro time delay can also be significant, i.e. $\delta t \sim 10^3 \text{ s} \left(\frac{M}{10^8 M_{\odot}} \right)$ as we will discuss in [38]. The central BH may also produce Lidov-Kozai oscillations, increasing the binary’s eccentricity [68, 69].

Besides the merger remnant’s emission in optical, X-rays from accretion onto the binary components and radio flares from jets are expected. Following [40], we find both effects difficult to observe even with future telescopes (e.g. Athena+, Square Kilometer Array) [38].

Acknowledgments. We acknowledge financial support from the European Union’s H2020 ERC Consolidator Grants “GRavity from Astrophysical to Microscopic Scales”, grant agreement no. GRAMS-815673 (to E.B.), and “Binary Massive Black Hole Astrophysics”, grant agreement no. BMAssive-818691 (to A.S.); from the Swiss National Science

Foundation; from the French space agency CNES in the framework of the LISA mission; from the European Union’s H2020 ERC, Starting Grant agreement no. DarkGRA–757480 (to P.P.); from the MIUR PRIN and FARE programmes (GW-NEXT, CUP: B84I20000100001, to P.P.). We thank I. Bartos, J.-M. Ezquiaga, J. Calderon Bustillo, and especially T. Dal Canton for insightful comments.

-
- [1] R. Abbott *et al.* (LIGO Scientific, Virgo), *Phys. Rev. Lett.* **125**, 101102 (2020), arXiv:2009.01075 [gr-qc].
 - [2] R. Abbott *et al.* (LIGO Scientific, Virgo), *Astrophys. J. Lett.* **900**, L13 (2020), arXiv:2009.01190 [astro-ph.HE].
 - [3] S. E. Woosley, A. Heger, and T. A. Weaver, *Reviews of Modern Physics* **74**, 1015 (2002).
 - [4] A. Heger, C. L. Fryer, S. E. Woosley, N. Langer, and D. H. Hartmann, *The Astrophysical Journal* **591**, 288 (2003), arXiv:astro-ph/0212469 [astro-ph].
 - [5] R. Farmer, M. Renzo, S. E. de Mink, P. Marchant, and S. Justham, *The Astrophysical Journal* **887**, 53 (2019), arXiv:1910.12874 [astro-ph.SR].
 - [6] D. Gerosa and E. Berti, *Phys. Rev. D* **95**, 124046 (2017), arXiv:1703.06223 [gr-qc].
 - [7] C. L. Rodriguez, M. Zevin, P. Amaro-Seoane, S. Chatterjee, K. Kremer, F. A. Rasio, and C. S. Ye, *Phys. Rev. D* **100**, 043027 (2019), arXiv:1906.10260 [astro-ph.HE].
 - [8] G. Fragione, A. Loeb, and F. A. Rasio, arXiv e-prints, arXiv:2009.05065 (2020), arXiv:2009.05065 [astro-ph.GA].
 - [9] Y. Levin, *Mon. Not. R. Astron. Soc* **374**, 515 (2007), arXiv:astro-ph/0603583 [astro-ph].
 - [10] B. McKernan, K. E. S. Ford, R. O’Shaughnessy, and D. Wysocki, *Mon. Not. R. Astron. Soc* **494**, 1203 (2020), arXiv:1907.04356 [astro-ph.HE].
 - [11] H. Tagawa, Z. Haiman, and B. Kocsis, *The Astrophysical Journal* **898**, 25 (2020), arXiv:1912.08218 [astro-ph.GA].
 - [12] I. Bartos, B. Kocsis, Z. Haiman, and S. Márka, *Astrophys. J.* **835**, 165 (2017), arXiv:1602.03831 [astro-ph.HE].
 - [13] Y. Yang, I. Bartos, Z. Haiman, B. Kocsis, Z. Marka, N. Stone, and S. Marka, *Astrophys. J.* **876**, 122 (2019), arXiv:1903.01405 [astro-ph.HE].
 - [14] T. Kinugawa, T. Nakamura, and H. Nakano, arXiv e-prints, arXiv:2009.06922 (2020), arXiv:2009.06922 [astro-ph.HE].
 - [15] T. Kinugawa, T. Nakamura, and H. Nakano, (2020), arXiv:2009.06922v1.
 - [16] M. Safarzadeh and Z. Haiman, (2020), arXiv:2009.09320 [astro-ph.HE].
 - [17] J. Sakstein, D. Croon, S. D. McDermott, M. C. Straight, and E. J. Baxter, (2020), arXiv:2009.01213 [gr-qc].
 - [18] V. De Luca, V. Desjacques, G. Franciolini, P. Pani, and A. Riotto, (2020), arXiv:2009.01728 [astro-ph.CO].
 - [19] J. Calderón Bustillo, N. Sanchis-Gual, A. Torres-Forné, J. A. Font, A. Vajpeyi, R. Smith, C. Herdeiro, E. Radu, and S. H. W. Leong, arXiv e-prints, arXiv:2009.05376 (2020), arXiv:2009.05376 [gr-qc].
 - [20] J. W. Moffat, arXiv e-prints, arXiv:2009.04360 (2020), arXiv:2009.04360 [gr-qc].
 - [21] M. Fishbach and D. E. Holz, arXiv e-prints, arXiv:2009.05472 (2020), arXiv:2009.05472 [astro-ph.HE].
 - [22] V. Gayathri, J. Healy, J. Lange, B. O’Brien, M. Szczepanczyk, I. Bartos, M. Campanelli, S. Klimentko, C. Lousto, and

- R. O’Shaughnessy, arXiv e-prints , arXiv:2009.05461 (2020), arXiv:2009.05461 [astro-ph.HE].
- [23] I. M. Romero-Shaw, P. D. Lasky, E. Thrane, and J. Calderon Bustillo, arXiv e-prints , arXiv:2009.04771 (2020), arXiv:2009.04771 [astro-ph.HE].
- [24] J. Calderón Bustillo, N. Sanchis-Gual, A. Torres-Forné, and J. A. Font, (2020), arXiv:2009.01066 [gr-qc].
- [25] M. Graham *et al.*, *Phys. Rev. Lett.* **124**, 251102 (2020), arXiv:2006.14122 [astro-ph.HE].
- [26] V. Connaughton *et al.*, *Astrophys. J. Lett.* **826**, L6 (2016), arXiv:1602.03920 [astro-ph.HE].
- [27] V. Savchenko *et al.*, *Astrophys. J. Lett.* **820**, L36 (2016), arXiv:1602.04180 [astro-ph.HE].
- [28] J. M. Bellovary, M.-M. Mac Low, B. McKernan, and K. E. S. Ford, *The Astrophysical Journal* **819**, L17 (2016), arXiv:1511.00005 [astro-ph.GA].
- [29] G. Ashton, K. Ackley, I. M. n. Hernandez, and B. Piotrkowski, (2020), arXiv:2009.12346 [astro-ph.HE].
- [30] P. Amaro-Seoane *et al.* (LISA), (2017), arXiv:1702.00786 [astro-ph.IM].
- [31] A. Sesana, *Phys. Rev. Lett.* **116**, 231102 (2016), arXiv:1602.06951 [gr-qc].
- [32] K. Jani, D. Shoemaker, and C. Cutler, *Nature Astronomy* **4**, 260 (2019), arXiv:1908.04985 [gr-qc].
- [33] A. Toubiana, S. Marsat, S. Babak, J. Baker, and T. Dal Canton, (2020), arXiv:2007.08544 [gr-qc].
- [34] E. Barausse, N. Yunes, and K. Chamberlain, *Phys. Rev. Lett.* **116**, 241104 (2016), arXiv:1603.04075 [gr-qc].
- [35] S. Vitale, *Physical Review Letters* **117** (2016), 10.1103/physrevlett.117.051102.
- [36] A. Toubiana, S. Marsat, S. Babak, E. Barausse, and J. Baker, *Phys. Rev. D* **101**, 104038 (2020), arXiv:2004.03626 [gr-qc].
- [37] E. Barausse, V. Cardoso, and P. Pani, *Phys. Rev. D* **89**, 104059 (2014), arXiv:1404.7149 [gr-qc].
- [38] A. Toubiana *et al.*, (In preparation).
- [39] J. M. Ezquiaga and D. E. Holz, (2020), arXiv:2006.02211 [astro-ph.HE].
- [40] A. Caputo, L. Sberna, A. Toubiana, S. Babak, E. Barausse, S. Marsat, and P. Pani, *Astrophys. J.* **892**, 90 (2020), arXiv:2001.03620 [astro-ph.HE].
- [41] C. Bonvin, C. Caprini, R. Sturani, and N. Tamanini, *Phys. Rev. D* **95**, 044029 (2017), arXiv:1609.08093 [astro-ph.CO].
- [42] K. Inayoshi, N. Tamanini, C. Caprini, and Z. Haiman, *Phys. Rev. D* **96**, 063014 (2017), arXiv:1702.06529 [astro-ph.HE].
- [43] N. Tamanini, A. Klein, C. Bonvin, E. Barausse, and C. Caprini, *Phys. Rev. D* **101**, 063002 (2020), arXiv:1907.02018 [astro-ph.IM].
- [44] V. Cardoso and A. Maselli, (2019), arXiv:1909.05870 [astro-ph.HE].
- [45] B. Abbott *et al.* (LIGO Scientific, Virgo), *Phys. Rev. Lett.* **116**, 221101 (2016), [Erratum: Phys.Rev.Lett. 121, 129902 (2018)], arXiv:1602.03841 [gr-qc].
- [46] H. Kim and W.-T. Kim, *Astrophys. J.* **665**, 432 (2007), arXiv:0705.0084 [astro-ph].
- [47] B. Kocsis, N. Yunes, and A. Loeb, *Phys. Rev. D* **84**, 024032 (2011), arXiv:1104.2322 [astro-ph.GA].
- [48] J. Frank, A. King, and D. J. Raine, *Accretion Power in Astrophysics, by Juhan Frank and Andrew King and Derek Raine, pp. 398. ISBN 0521620538. Cambridge, UK: Cambridge University Press, February 2002.* (2002) p. 398.
- [49] E. C. Ostriker, *Astrophys. J.* **513**, 252 (1999), arXiv:astro-ph/9810324 [astro-ph].
- [50] E. Barausse, *Mon. Not. Roy. Astron. Soc.* **382**, 826 (2007), arXiv:0709.0211 [astro-ph].
- [51] C. F. Macedo, P. Pani, V. Cardoso, and L. C. Crispino, *Astrophys. J.* **774**, 48 (2013), arXiv:1302.2646 [gr-qc].
- [52] H. Kim, W.-T. Kim, and F. J. Sanchez-Salcedo, *Astrophys. J.* **679**, L33 (2008), arXiv:0804.2010 [astro-ph].
- [53] V. Varma, S. E. Field, M. A. Scheel, J. Blackman, D. Gerosa, L. C. Stein, L. E. Kidder, and H. P. Pfeiffer, *Phys. Rev. Research.* **1**, 033015 (2019), arXiv:1905.09300 [gr-qc].
- [54] S. Husa, S. Khan, M. Hannam, M. Pürrer, F. Ohme, X. Jiménez Forteza, and A. Bohé, *Phys. Rev. D* **93**, 044006 (2016), arXiv:1508.07250 [gr-qc].
- [55] S. Khan, S. Husa, M. Hannam, F. Ohme, M. Pürrer, X. J. Forteza, and A. Bohé, *Phys. Rev. D* **93**, 044007 (2016).
- [56] S. Marsat and J. G. Baker, (2018), arXiv:1806.10734 [gr-qc].
- [57] S. Marsat, J. G. Baker, and T. Dal Canton, (2020), arXiv:2003.00357 [gr-qc].
- [58] X. Li, P. Chang, Y. Levin, C. D. Matzner, and P. J. Armitage, *Mon. Not. Roy. Astron. Soc.* **494**, 2327 (2020), arXiv:1912.06864 [astro-ph.HE].
- [59] R. L. Karandikar, *Sadhana* **31**, 81 (2006).
- [60] D. J. D’Orazio and A. Loeb, *Phys. Rev. D* **101**, 083031 (2020), arXiv:1910.02966 [astro-ph.HE].
- [61] D. J. D’Orazio and R. Di Stefano, *Mon. Not. Roy. Astron. Soc.* **474**, 2975 (2018), arXiv:1707.02335 [astro-ph.HE].
- [62] P. Schneider, J. Ehlers, and E. E. Falco, *Gravitational Lenses* (Springer Verlag, 1992).
- [63] R. Takahashi and T. Nakamura, *Astrophys. J.* **595**, 1039 (2003), arXiv:astro-ph/0305055.
- [64] N. Yunes, K. Yagi, and F. Pretorius, *Phys. Rev. D* **94**, 084002 (2016), arXiv:1603.08955 [gr-qc].
- [65] A. Gruzinov, Y. Levin, and C. D. Matzner, (2019), arXiv:1906.01186 [astro-ph.HE].
- [66] H. Yu and Y. Chen, (2020), arXiv:2009.02579 [gr-qc].
- [67] Y. Fang, X. Chen, and Q.-G. Huang, *The Astrophysical Journal* **887**, 210 (2019), arXiv:1908.01443 [astro-ph.HE].
- [68] M. L. Lidov, *Planet. Space Sci.* **9**, 719 (1962).
- [69] Y. Kozai, *Astron. J.* **67**, 591 (1962).